



Haplotype-resolved de novo assembly using phased assembly graphs with hifiasm

Haoyu Cheng^{1,2}, Gregory T. Concepcion³, Xiaowen Feng^{1,2}, Haowen Zhang⁴ and Heng Li^{1,2}✉

Haplotype-resolved de novo assembly is the ultimate solution to the study of sequence variations in a genome. However, existing algorithms either collapse heterozygous alleles into one consensus copy or fail to cleanly separate the haplotypes to produce high-quality phased assemblies. Here we describe hifiasm, a de novo assembler that takes advantage of long high-fidelity sequence reads to faithfully represent the haplotype information in a phased assembly graph. Unlike other graph-based assemblers that only aim to maintain the contiguity of one haplotype, hifiasm strives to preserve the contiguity of all haplotypes. This feature enables the development of a graph trio binning algorithm that greatly advances over standard trio binning. On three human and five nonhuman datasets, including California redwood with a ~30-Gb hexaploid genome, we show that hifiasm frequently delivers better assemblies than existing tools and consistently outperforms others on haplotype-resolved assembly.

De novo genome assembly is the most comprehensive method that provides unbiased insight to DNA sequences. With the rapid advances in long-read sequencing technologies such as Pacific Biosciences (PacBio) and Oxford Nanopore (ONT), many long-read assemblers have been developed to tackle this essential computational problem. Most of them^{1–9} collapse different homologous haplotypes into a consensus representation with heterozygous alleles frequently switching in the consensus. This approach works well for inbred samples that are nearly homozygous but necessarily misses half of the genetic information in a diploid genome. To solve this problem, Falcon-Unzip¹⁰ recovers heterozygous alleles by ‘unzipping’ them in an initial collapsed assembly. It produces a pair of assemblies, one primary assembly representing a mosaic of homologous haplotypes, and one alternate assembly composed of short haplotype-specific contigs (haplotigs) for alleles absent from the primary assembly. The alternate assembly is often fragmented and does not represent a complete haplotype, making it less useful in practice. In addition, starting from a collapsed assembly, Falcon-Unzip may not recover highly heterozygous regions that are not properly collapsed in the initial assembly. Trio binning¹¹ addresses these issues by globally partitioning long reads upfront with parental short reads and then performing two separate assemblies on the partitioned reads. This strategy works well for samples with high heterozygosity, but for a human sample sequenced with noisy long reads, it only produces fragmented assemblies with ~1.2-Mb contigs.

A great challenge to the assembly of heterozygous samples is caused by the 5–15% sequencing error rate of older long reads. With this high error rate, it is difficult to distinguish errors from heterozygotes occurring at a rate of <0.1% in humans. The recent availability of high-fidelity (HiFi) reads¹² produced by PacBio has changed the equation. Generated from the consensus of multiple sequences of the same DNA molecule, HiFi reads have a much lower error rate of <1%. With HiFi, standard trio binning can produce contigs of 17 Mb¹². Recent works relying on high-throughput chromosomal confirmation capture (Hi-C) or strand sequencing (Strand-seq) read binning^{13,14} can achieve better contiguity and phasing accuracy. These pre-binning algorithms all use short *k*-mers or short reads to

partition HiFi reads^{15,16}. They may not identify haplotype-specific markers in complex regions and result in wrong read partitions, which will negatively affect the assembly, as shown later. In addition, both Hi-C and Strand-seq binning start with a collapsed assembly and have the same issues as Falcon-Unzip.

In 2012, we reasoned¹⁷ that a perfectly constructed unitig graph with read information is a lossless representation of single-end reads. Because this graph is lossless, we can compress input reads into a unitig graph and perform phasing later. This should maximize the power of long HiFi reads. Developed in parallel to our work, HiCanu¹⁸ follows a similar rationale and can produce Falcon-Unzip-style primary/alternate assemblies better than other assemblers especially around segmental duplications. However, HiCanu only tries to keep the contiguity of one parental haplotype and often breaks the contiguity of the other haplotype. When we separate parental haplotypes, these breakpoints will lead to fragmented haplotype-resolved assemblies.

Here we present hifiasm, an assembler for HiFi reads that generates a well-connected assembly graph and produces better assemblies in practice. We first provide an overview of the hifiasm algorithm, compare it to other assemblers for partially phased assemblies and then explain and evaluate the haplotype-resolved assembly algorithm used by hifiasm.

Results

Overview of the hifiasm algorithm. The first few steps of hifiasm broadly resemble the workflow of early long-read assemblers^{1,2} (Fig. 1). Hifiasm performs all-versus-all read overlap alignment and then corrects sequencing errors. Given a target read to be corrected, hifiasm inspects the alignment of reads overlapping with the target read. A position on the target read is said to be informative if there are two types of A/C/G/T bases (gaps ignored) at the position in the alignment, and each type is supported by at least three reads. A read overlapping with the target read is inconsistent with the target if there are informative positions in the overlap and the read is not identical to the target read across all these positions; accordingly, the overlap between this and the target read is inconsistent.

¹Department of Data Science, Dana-Farber Cancer Institute, Boston, MA, USA. ²Department of Biomedical Informatics, Harvard Medical School, Boston, MA, USA. ³Pacific Biosciences, Menlo Park, CA, USA. ⁴School of Computational Science and Engineering, Georgia Institute of Technology, Atlanta, GA, USA. ✉e-mail: hli@jimmy.harvard.edu

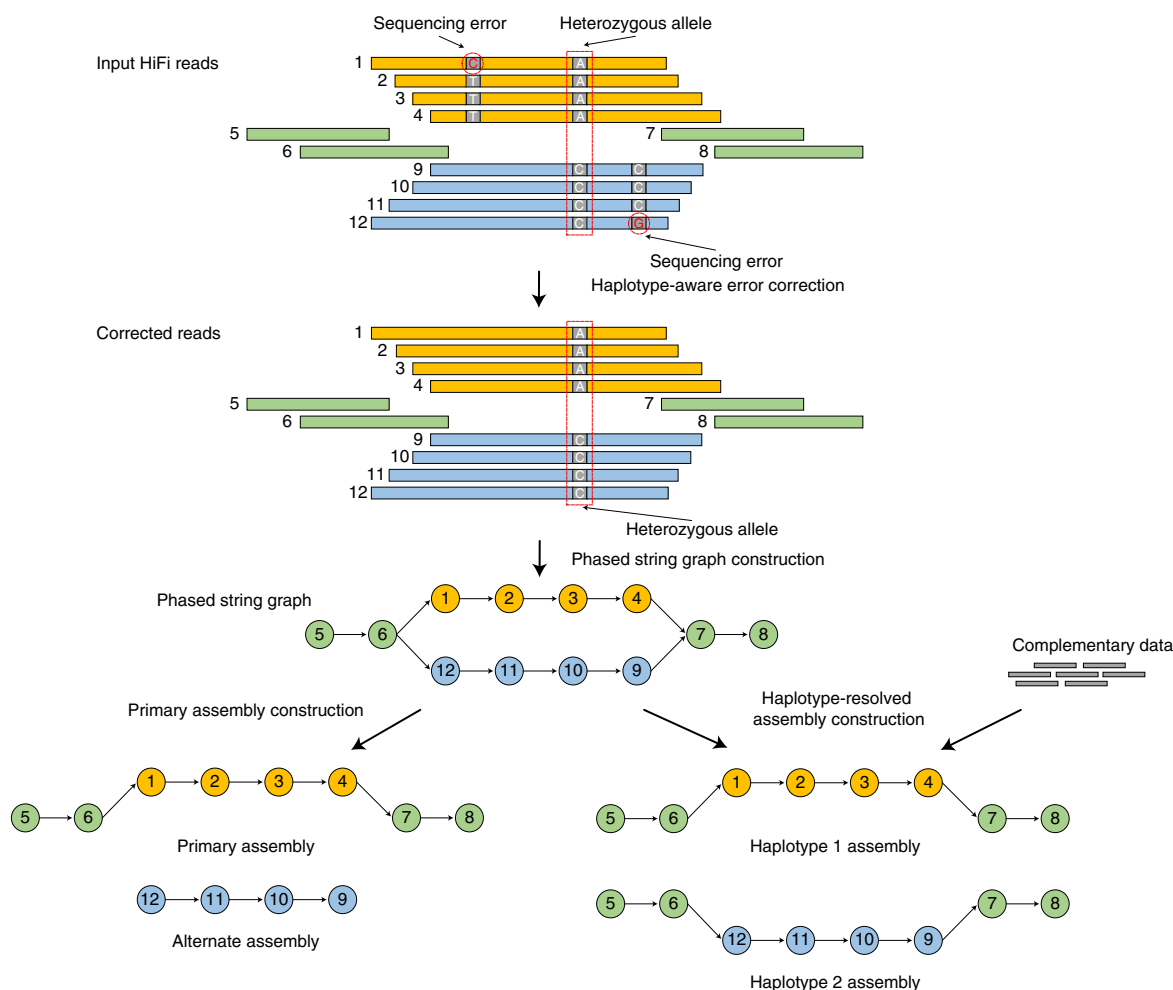


Fig. 1 | Outline of the hifiasm algorithm. Orange and blue bars represent the reads with heterozygous alleles carrying local phasing information, while green bars come from the homozygous regions without any heterozygous alleles. In the phased string graph, a vertex corresponds to the HiFi read with the same ID, and an edge between two vertices indicates that their corresponding reads are overlapped with each other. Hifiasm first performs haplotype-aware error correction to correct sequence errors but keep heterozygous alleles, and then builds a phased assembly graph with local phasing information from the corrected reads. Only the reads coming from the same haplotype are connected in the phased assembly graph. With complementary data providing global phasing information, hifiasm generates a completely phased assembly for each haplotype from the graph. Hifiasm also can generate an unphased primary assembly only with HiFi reads. This unphased primary assembly represents phased blocks (regions) that are resolvable with HiFi reads, but does not preserve phasing information between two phased blocks.

Inconsistent reads theoretically originate from a haplotype different from the target read. Hifiasm only uses consistent reads to correct the target read.

Hifiasm performs three rounds of error correction by default. It then does overlap alignment again and builds a string graph¹⁹ where a vertex is an oriented read and an edge is a consistent overlap. After transitive reduction, a pair of heterozygous alleles will be represented by a ‘bubble’ in the string graph (Fig. 1). No information is lost. If there are no additional data, hifiasm arbitrarily selects one side of each bubble and outputs a primary assembly similar to Falcon-Unzip and HiCanu. For a heterozygous genome, the primary assembly generated at this step may still contain haplotigs from more than one homologous haplotype. HiCanu relies on third-party tools such as *purge_dups*²⁰ to remove redundant haplotigs. Hifiasm natively implements a variant of the *purge_dups* algorithm. This simplifies the assembly pipeline.

If parents of the sample are also sequenced, hifiasm can use *k*-mer trio binning¹¹ to label corrected reads in the string graph. In this case, hifiasm effectively discards the maternal unitigs to generate

the paternal assembly, and vice versa. This graph-based trio binning may go through regions heterozygous in all three samples in the trio and is more robust to the mislabeling of reads. We will explain the advantage of hifiasm binning in a later section.

Assembling homozygous nonhuman genomes. We first evaluated hifiasm (v0.12) along with Falcon-Unzip¹⁰ (v1.8.1), Peregrine⁶ (v0.1.6.1) and HiCanu¹⁸ (v2.1) on two inbred samples²¹, including the C57BL/6J strain of *Mus musculus* (mouse) and the B73 strain of *Zea mays* (maize). All assemblers produced long contigs for mouse (Table 1). To evaluate how often assemblers collapse paralogous regions and produce misassemblies, we mapped HiFi reads to each assembly, extracted apparently heterozygous single-nucleotide polymorphism (SNPs) at high coverage and clustered them into longer regions (Methods). These regions correspond to collapsed misassemblies. We identified 4 such misassemblies in the HiCanu assembly, 6 in hifiasm and more than 100 in both Falcon and Peregrine. HiCanu performs best on this metric, although its contig N50 length is the shortest.

Table 1 | Statistics of nonhuman assemblies

Dataset	Assembler	Size (Gb)	N50 (Mb)	NG50 (Mb)	Alternate size (Gb)	Completeness (asmgene or BUSCO)	
						Complete (%)	Duplicated (%)
<i>M. musculus</i> (25×)	Hifiasm	2.610	21.1	20.6	0.044	99.73	0.23
	HiCanu	2.594	16.0	14.8	0.077	99.68	0.22
	Peregrine	2.578	17.9	17.0	0.029	99.56	0.21
	Falcon	2.559	19.3	16.7	0.025	99.49	0.14
<i>Z. mays</i> (22×)	Hifiasm	2.190	37.5	37.5	0.095	99.85	0.17
	HiCanu	2.145	27.1	24.1	0.040	99.84	0.13
	Peregrine	2.205	10.1	10.2	0.038	99.88	0.26
	Falcon	2.132	9.5	9.3	0.016	99.77	0.17
<i>F. × ananassa</i> (36×)	Hifiasm (purge)	0.829	17.6	17.6	0.458	98.45	93.43
	HiCanu	1.044	8.4	9.8	0.295	98.08	92.94
	HiCanu (purge)	0.411	10.5	0.0	0.928	96.78	55.08
	Peregrine	0.930	5.5	6.7	0.260	98.33	91.70
	Falcon	0.971	5.4	7.3	0.213	98.27	92.81
<i>R. muscosa</i> (~29×)	Hifiasm (purge)	9.664	9.1		7.208	66.61	1.70
	HiCanu	9.645	5.2		6.361	65.54	3.92
	Peregrine	9.415	0.9		2.936	66.84	1.72
<i>S. sempervirens</i> (~33×)	Hifiasm (purge)	35.310	5.5		15.757	61.31	39.42
	Peregrine	35.662	0.8			63.20	35.93

HiCanu (purge) applies `purge_dups` to a HiCanu assembly. Hifiasm (purge) enables the built-in `purge_dups` equivalent strategy. The N50/NG50 of an assembly is defined as the sequence length of the shortest contig at 50% of the total assembly/genome size. To calculate the NG50, a genome size of 2730.9 Mb (AC:GCF_000001635.20), 2182.1 Mb (AC:GCA_902167145.1) and 813.4 Mb²² was used for *M. musculus*, *Z. mays* and *F. × ananassa*, respectively. The genome size is unknown for *R. muscosa* and *S. sempervirens*. 'Alternate size' is the total length of the alternate assembly. The reference-based asmgene method²⁹ was used to evaluate the gene completeness of *M. musculus* and *Z. mays*, which have high-quality reference genomes. For these two samples, 'complete' gives the percentage of single-copy genes in the reference genome (one unique mapping at ≥97% identity) that are mapped at ≥97% identity to the assembly; 'duplicated' gives the percentage of reference single-copy genes that become multicopy genes in the assembly. The BUSCO Embryophyta dataset was used to evaluate the gene completeness of *F. × ananassa* and *S. sempervirens*; the Tetrapoda dataset was used for *R. muscosa*. BUSCO scores of all samples are available in Supplementary Table 7.

For the repeat-rich maize genome, hifiasm and HiCanu generated longer contigs and again produced much fewer collapsed misassemblies. There were 3 collapsed misassemblies in the hifiasm assembly and 9 in HiCanu, versus more than 100 in Falcon and Peregrine. Hifiasm and HiCanu perform better presumably because they can more effectively resolve repeats by requiring near-perfect overlap¹⁸.

Assembling heterozygous nonhuman genomes. Because most natural samples are heterozygous, we next evaluated the assemblers on three heterozygous datasets from *Fragaria × ananassa* (garden strawberry), *Rana muscosa* (mountain yellow-legged frog) and *Sequoia sempervirens* (California redwood). These samples are more challenging to assemble. *F. × ananassa* has an allopolyploid genome estimated to be 813.4 Mb in size²². All assemblers achieved a total assembly of ~1.2 Gb, including both primary and alternate contigs. However, they resolved the primary assembly differently. Hifiasm resulted in a primary assembly of similar size to the published genome. BUSCO²³ regarded most single-copy genes to be duplicated, consistent with the previous observation²². HiCanu assigned most contigs to the primary assembly. Applying `purge_dups`²⁰ over-compressed the assembly and reduced the BUSCO completeness by 5%. Falcon-Unzip and Peregrine were somewhat between hifiasm and HiCanu. The varying primary assembly sizes highlight the difficulty in assembling polyploid genomes. On the other hand, all HiFi assemblies here have much longer contigs than the published assembly (N50 > 5 Mb versus 580 kb). HiFi enables better assembly.

R. muscosa is hard to assemble for its large genome size. We failed to run Falcon-Unzip for this sample using its released version. We did not apply `purge_dups` to the HiCanu assembly as it could

not finish in 15 d. Without the purging step, the HiCanu assembly contained a higher rate of duplicated genes. The N50 of the hifiasm assembly was almost twice as long as the HiCanu assembly.

S. sempervirens poses an even greater challenge to assembly with a much larger hexaploid genome. Hifiasm took 875-Gb reads as input and produced a 35.6-Gb assembly in 3 d over 80 CPU threads using ~700 GB of memory at the peak (Supplementary Table 10). The flow cytometric estimate of the full hexaploid genome is 62.8 Gb in size²⁴. Our assembly is about half of that. Peregrine achieved a 35.6-Gb assembly as well. Its BUSCO score was 1.9% better than the hifiasm assembly. Peregrine ran for 15 d on a computer cluster; it was slower and its assembly more fragmented. Hifiasm overall performed better on large genomes.

Primary assembly of human genomes. We next evaluated hifiasm and other assemblers on three human datasets (Table 2). We introduced two new metrics, 'multicopy genes retained' and 'resolved bacterial artificial chromosomes (BACs)', to evaluate how assemblers resolve difficult genomic regions such as long segmental duplications. If an assembler breaks contigs at such regions or misassembles the regions, the resulting assembly will lose multicopy genes and/or lead to fragmented BAC-to-contig alignment.

CHM13 is a homozygous cell line, similar to *M. musculus* and *Z. mays*. The telomere-to-telomere (T2T) consortium produced a near-complete assembly for this sample with multiple data types and manual curation. Taking the T2T assembly as the ground truth, QUAST²⁵ reported 349 misassemblies in the HiCanu assembly, 476 in the hifiasm assembly and more than 1,500 misassemblies in others (Supplementary Table 1). HiCanu performed best regarding the number of misassemblies. Nonetheless, it had a shorter NG50,

Table 2 | Statistics of human primary assemblies

Dataset	Assembly	Size (Gb)	NG50 (Mb)	NGA50 (Mb)	QV	Multicopy genes retained (%)	Resolved BACs (%)	Gene completeness (asmgene)	
								Complete (%)	Duplicated (%)
CHM13 (HiFi 32x)	Hifiasm	3.052	88.9	86.7	54.2	99.7	98.8	99.97	0.05
	HiCanu	3.037	69.7	67.9	54.1	98.9	97.6	99.97	0.04
	Peregrine	2.990	37.8	33.4	43.8	51.1	39.7	99.64	0.16
	Falcon	2.862	27.1	21.8	50.1	30.2	34.2	99.47	0.03
CHM13 (ONT 120x)	Canu	2.936	80.0	47.3	32.7	76.9	86.7	99.30	0.10
	Flye	2.900	37.5	34.0	33.5	54.7	60.6	99.22	0.11
	Shasta	2.820	41.3	33.4	30.4	26.7	27.9	98.05	0.01
HG00733 (HiFi 33x)	Hifiasm (purge)	3.043	68.3	55.3	49.9	74.6	80.4	99.07	0.39
	HiCanu (purge)	2.921	40.5	34.2	50.5	55.2	65.9	98.47	0.32
	Peregrine	3.035	30.1	30.1	40.5	37.2	38.5	98.70	0.31
	Falcon	2.861	24.4	23.2	46.3	33.6	38.0	96.51	0.15
HG00733 (ONT 50x)	Canu	2.923	41.1	36.6	29.5	54.6	69.3	98.32	0.66
	Flye	2.890	26.7	25.4	29.9	34.2	44.7	97.88	0.20
	Shasta	2.805	21.2	20.8	30.0	17.0	22.9	97.19	0.05
HG002 (HiFi 36x)	Hifiasm (purge)	3.067	98.2	64.1	51.5	75.8		99.26	0.32
	HiCanu (purge)	2.953	48.3	39.4	52.1	59.7		98.71	0.18
	Peregrine	3.081	33.4	32.5	41.3	42.5		99.14	0.36
	Falcon	2.955	30.4	29.0	46.7	36.6		99.00	0.20

Polished ONT assemblies were generated by the Shasta developers⁸. HiCanu and hifiasm were run without duplication purging for the homozygous CHM13 cell line and with purging for the heterozygous HG00733 and HG002 cell lines. The NGA50 of an assembly is the length of the correctly aligned block at 50% of the total reference genome size, which is assumed to be 3.1 Gb. It was calculated based on the minigraph²⁸ contig-to-reference alignment. QV is the Phred-scaled contig base error rate measured by comparing 31-mers in contigs to 31-mers in short reads from the same sample. 'Multicopy genes retained', reported by asmgene (Methods), is the percentage of multicopy genes in the reference genome (multiple mapping positions at $\geq 99\%$ sequence identity) that remain multicopy genes in the assembly. A BAC is resolved if 99.5% of its bases can be mapped to the assembly. There were 330 CHM13-specific BACs excluding those not resolved by the T2T assembly, and there were 179 HG00733-specific BACs. HG002 does not have BAC data. GRCh38 was used as the reference genome for HG00733 and HG002, and the T2T CHM13 assembly (v0.9) was used as the reference for CHM13.

missed more multicopy genes and resolved fewer BACs in comparison to hifiasm. Hifiasm and HiCanu are broadly comparable. Both of them performed better than Peregrine, Falcon and ONT assemblies on all metrics by a large margin.

QUAST often takes structural variations as misassemblies. Taking GRCh38 as the reference, it reported 23,541 misassemblies for the T2T assembly, greatly overestimating assembly errors. We thus did not apply QUAST to HG00733 and HG002 where the ground truth is missing. Instead, we inferred NGA50 based on minigraph alignment that can go through most structural variations (Table 2). This more accurately measures large-scale misassemblies.

For these two heterozygous samples, HiCanu produced primary assemblies with several hundred megabases of heterozygous regions represented twice. We thus ran `purge_dups`²⁰ to remove these falsely duplicated regions in the primary assembly. We tried a few `purge_dups` settings, including the default, and chose the one that gave the best primary assembly. Hifiasm can identify and remove falsely duplicated regions by inspecting inconsistent read overlaps between them. The other assemblers collapsed most heterozygous regions during assembly. They do not need additional tools like `purge_dups` either.

For HG00733 and HG002, hifiasm and HiCanu consistently outperformed other assemblers. The hifiasm assembly was more complete and resolved more difficult regions than HiCanu. This

difference probably has more to do with the duplicate purging algorithm than with the capability of the assembler. Nonetheless, this observation suggests it is easier to produce a high-quality primary assembly with hifiasm.

On running time, hifiasm ran for 7–9 wall-clock hours over 48 threads (Supplementary Table 10). The peak memory was below 150 GB. Peregrine was about twice as fast for human assembly but used more memory. HiCanu was about 7–8 times as slow as hifiasm using the same machine. Falcon was the slowest.

Improving haplotype-resolved assembly. A major issue with trio binning is that a fraction of heterozygous reads cannot be unambiguously partitioned to parental haplotypes: if both parents are heterozygous at a locus, a child read will not harbor informative *k*-mers and cannot be uniquely assigned to a parental haplotype; if, say, the father is heterozygous at a locus and the mother is homozygous, reads from the maternal haplotype cannot be partitioned either. With standard trio binning, heterozygous reads that cannot be partitioned will be used in both parental assemblies. As a result, both alleles may be present in one haplotype assembly and lead to false duplications. Standard trio binning is unable to cleanly separate the two parental haplotypes.

Hifiasm draws power from HiFi read phasing in addition to trio binning. It does not partition reads upfront; it only labels reads in

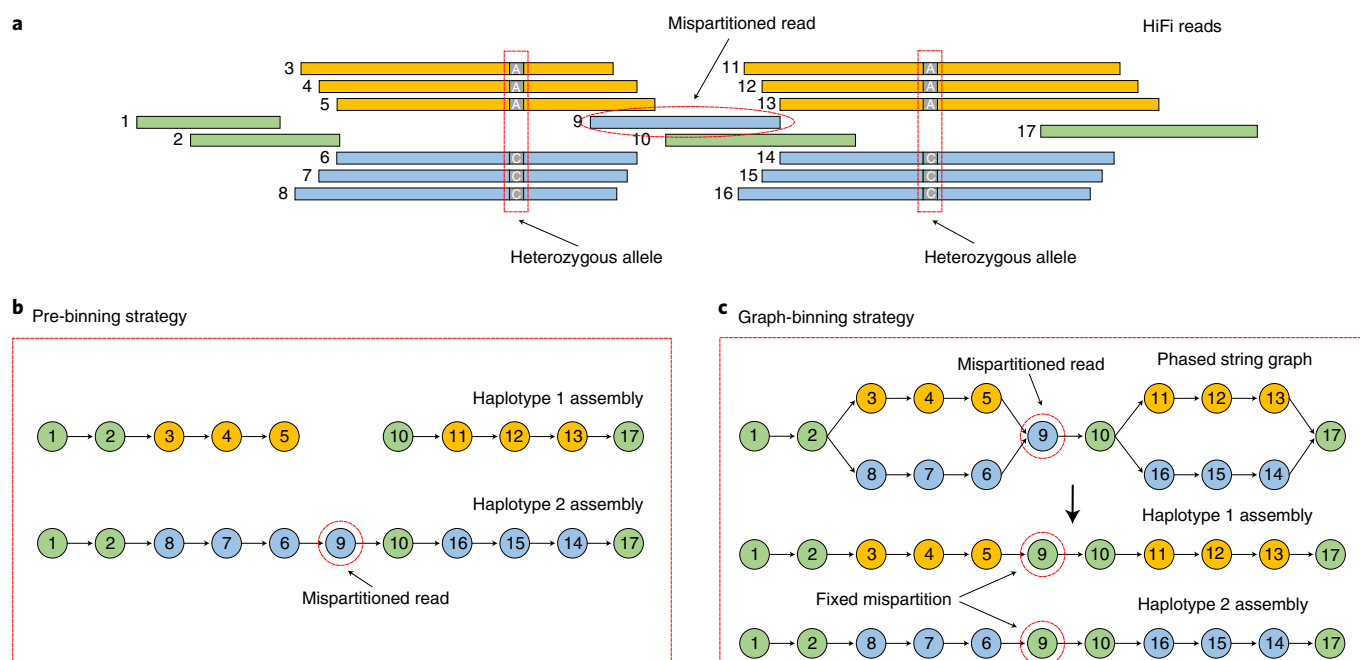


Fig. 2 | Effect of false read binning. **a**, A set of reads with global phasing information provided by the complementary data. Reads in orange and reads in blue are specifically partitioned into haplotype 1 and haplotype 2, respectively. The remaining reads in green are partitioned into both haplotypes. Read 9 without heterozygous alleles is mispartitioned into haplotype 2, instead of to both haplotypes. **b**, Pre-binning assemblies produced by current methods that independently assemble two haplotypes. Haplotype 1 is broken into two contigs due to the mispartitioning of read 9. **c**, Hifiasm fixes the mispartitioning by the local phasing information in the phased assembly graph. It can identify that read 9 does not have heterozygous alleles, so that read 9 should be partitioned into both haplotypes.

the string graph. In a long bubble representing a pair of heterozygous alleles, hifiasm may correctly phase it even if only a small fraction of reads are correctly labeled. This way hifiasm also rarely puts two parental alleles in one haplotype assembly.

Hi-C- or Strand-seq-based phasing^{13,14} can unambiguously phase most heterozygous reads and are naturally immune to false duplications. They, however, suffer from another issue shared by standard trio phasing: reads assigned to a wrong parental haplotype may break contigs (Fig. 2). By considering HiFi read phasing and the structure of the assembly graph, hifiasm may be able to identify and fix such binning errors.

Haplotype-resolved assembly of heterozygous human genomes.

To evaluate how well assemblers resolve both haplotypes, we applied a trio binning assembly to HG00733 and HG002. Hifiasm performs graph trio binning that partitions a diploid assembly graph to generate the final assembly. HiCanu performs standard trio binning¹¹ that partitions HiFi reads upfront and assembles the two parental partitions separately. Peregrine does not natively support trio binning. We fed the HiCanu-partitioned reads to Peregrine for assembly. For comparison, we also acquired a Strand-seq HG00733 assembly¹⁴ and a Hi-C HG00733 assembly¹³ that use the same HiFi reads but are supplemented with additional data types for phasing.

On both datasets, trio hifiasm missed fewer variants and emitted longer contigs with higher quality value (QV) and lower variant false discovery rate (FDR) than other assembly strategies (Table 3). The HiCanu contig NG50 was the shortest, which is probably caused by wrongly partitioned reads (Fig. 2) in combination with HiCanu's strict requirement of exact overlapping. By collapsing inexact overlaps, Peregrine is more robust to partition errors in certain cases and can achieve longer contigs. However, this comes with the cost of fewer resolved BACs and increased false negative rate (FNR). The Strand-seq and Hi-C assemblies also use Peregrine and are affected by false read partitions in the same way. These two assemblies were

not as good as hifiasm. It is not possible to get a good all-around assembly if we perform separate assemblies on prepartitioned reads.

The human leukocyte antigen region is highly heterozygous and enriched with complex variations. For HG002, we compared each assembly to the haplotype-resolved ground truth of the same sample²⁶ (Supplementary Table 9). While hifiasm fully reconstructed both haplotypes, HiCanu failed to assemble the paternal haplotypes, and peregrine likely introduced misassemblies in both haplotypes. These results are consistent with the BAC resolution of HG00733 assemblies (Table 3), showing that trio hifiasm can more effectively resolve hard regions.

Discussion

Hifiasm is a fast open-source de novo assembler specifically developed for HiFi reads. It mostly uses exact overlaps to construct the assembly graph and can separate different alleles or different copies of a segmental duplication involving a single segregating site. This greatly enhances its power for resolving near-identical, but not exactly identical, repeats and segmental duplications. In our evaluation, hifiasm consistently outperforms Falcon and Peregrine, which do not take the advantage of exact overlaps.

In comparison to HiCanu, which was developed in parallel to our work, hifiasm can generate a more complete assembly graph preserving all haplotypes more contiguously. This enabled us to implement a graph trio binning algorithm that can produce a haplotype-resolved assembly tripling the contig N50 of a trio HiCanu assembly. To our knowledge, hifiasm can generate overall the best haplotype-resolved human assemblies so far.

Our graph-binning algorithm can also work with reads labeled by Hi-C or Strand-seq binning that do not require parental data. However, because existing Hi-C or Strand-seq binning algorithms start with a collapsed assembly, they may not work well with highly heterozygous regions not represented well in the initial assembly. In our view, a better solution to pedigree-free phased assembly is

Table 3 | Statistics of haplotype-resolved human assemblies

Dataset	Assembly	Size (Gb)	QV	NG50 (Mb)	Multicopy genes retained (%)	Resolved BACs (%)	Switch error (%)	Hamming error (%)	FNR (%)	FDR (%)
HG00733	Hifiasm (trio)	6.071	49.9	34.9	84.0	95.5	0.08	0.22	2.43	
	HiCanu (trio)	6.079	49.2	10.6	84.3	90.5	0.04	0.04	4.78	
	Peregrine (trio)	5.938	42.2	19.1	37.6	39.7	0.10	0.23	12.34	
	Peregrine (Hi-C)	5.867	41.6	26.1	33.2	35.2	0.12	0.67	3.31	
	Peregrine (Strand-seq)	5.805	45.8	26.6	33.0	46.9	0.18	0.72	3.99	
HG002	Hifiasm (trio)	5.967	51.6	43.0	80.6		0.79	0.34	0.88	0.26
	HiCanu (trio)	6.003	50.4	12.1	80.4		0.75	0.19	1.57	0.32
	Peregrine (trio)	5.888	42.7	25.8	38.7		0.70	0.18	4.42	4.18

Parental assemblies were merged together for computing QV, NG50 and resolved BACs. Calculating NG50 assumes a diploid human genome size of 6.2 Gb. Phased variants were called with dipcall²⁹ for each pair of parental assemblies and compared to HG002 truth variants from The Genome in a Bottle (GIAB) consortium³⁰ or HG00733 phased SNPs from The Human Genome Structural Variation Consortium (HGSVC)³¹. Phasing switch error rate: the percentage of adjacent SNP pairs that are wrongly phased. Phasing hamming error rate: the percentage of SNP sites that are wrongly phased. FNR: the percentage of true variants that are missed in the assembly. FDR: the percentage of assembly-based variant calls that are not called in the truth data. RTG Tool's vcfeval³² was used for estimating variant FNR and FDR for HG002. For HG00733, FNR was estimated at heterozygous SNP sites only; FDR was not available because HGSVC does not provide confident regions. The percentage of 'multicopy genes retained' measures the percentage of multicopy genes in GRCh38 (multiple mapping positions at ≥99% sequence identity) that remain multicopy genes in the assembly, averaged between the two parental haplotypes. Gene completeness (asmgene) can be found in Supplementary Table 2.

to map Hi-C or Strand-seq data to the hifiasm assembly graph, group and order unitigs into chromosome-long scaffolds with the graph topology, and then phase heterozygous events along the scaffolds. We envision that haplotype-resolved assembly will become a common practice for both human and diploid nonhuman species, although haplotype-resolved assembly may remain challenging for polyploid plants in the near future.

Online content

Any methods, additional references, Nature Research reporting summaries, source data, extended data, supplementary information, acknowledgements, peer review information; details of author contributions and competing interests; and statements of data and code availability are available at <https://doi.org/10.1038/s41592-020-01056-5>.

Received: 26 June 2020; Accepted: 23 December 2020;
Published online: 1 February 2021

References

- Chin, C.-S. et al. Nonhybrid, finished microbial genome assemblies from long-read SMRT sequencing data. *Nat. Methods* **10**, 563–569 (2013).
- Berlin, K. et al. Assembling large genomes with single-molecule sequencing and locality-sensitive hashing. *Nat. Biotechnol.* **33**, 623–630 (2015).
- Li, H. Minimap and miniasm: fast mapping and de novo assembly for noisy long sequences. *Bioinformatics* **32**, 2103–2110 (2016).
- Koren, S. et al. Canu: scalable and accurate long-read assembly via adaptive *k*-mer weighting and repeat separation. *Genome Res.* **27**, 722–736 (2017).
- Kolmogorov, M., Yuan, J., Lin, Y. & Pevzner, P. A. Assembly of long, error-prone reads using repeat graphs. *Nat. Biotechnol.* **37**, 540–546 (2019).
- Chin, C.-S. & Khalak, A. Human genome assembly in 100 minutes. Preprint at *bioRxiv* <https://doi.org/10.1101/705616> (2019).
- Ruan, J. & Li, H. Fast and accurate long-read assembly with wtdbg2. *Nat. Methods* **17**, 155–158 (2020).
- Shafin, K. et al. Nanopore sequencing and the Shasta toolkit enable efficient de novo assembly of eleven human genomes. *Nat. Biotechnol.* **38**, 1044–1053 (2020).
- Chen, Y. et al. Efficient assembly of nanopore reads via highly accurate and intact error correction. *Nat. Commun.* **12**, 60 (2021).
- Chin, C.-S. et al. Phased diploid genome assembly with single-molecule real-time sequencing. *Nat. Methods* **13**, 1050–1054 (2016).
- Koren, S. et al. De novo assembly of haplotype-resolved genomes with trio binning. *Nat. Biotechnol.* **36**, 1174–1182 (2018).
- Wenger, A. M. et al. Accurate circular consensus long-read sequencing improves variant detection and assembly of a human genome. *Nat. Biotechnol.* **37**, 1155–1162 (2019).
- Garg, S. et al. Chromosome-scale, haplotype-resolved assembly of human genomes. *Nat. Biotechnol.* <https://doi.org/10.1038/s41587-020-0711-0> (2020).
- Porubsky, D. et al. Fully phased human genome assembly without parental data using single-cell strand sequencing and long reads. *Nat. Biotechnol.* <https://doi.org/10.1038/s41587-020-0719-5> (2020).
- Martin, M. et al. WhatsHap: fast and accurate read-based phasing. Preprint at *bioRxiv* <https://doi.org/10.1101/085050> (2016).
- Edge, P., Bafna, V. & Bansal, V. HapCUT2: robust and accurate haplotype assembly for diverse sequencing technologies. *Genome Res.* **27**, 801–812 (2017).
- Li, H. Exploring single-sample SNP and INDEL calling with whole-genome de novo assembly. *Bioinformatics* **28**, 1838–1844 (2012).
- Nurk, S. et al. HiCanu: accurate assembly of segmental duplications, satellites, and allelic variants from high-fidelity long reads. *Genome Res.* **30**, 1291–1305 (2020).
- Myers, E. W. The fragment assembly string graph. *Bioinformatics* **21**, ii79–ii85 (2005).
- Guan, D. et al. Identifying and removing haplotypic duplication in primary genome assemblies. *Bioinformatics* **36**, 2896–2898 (2020).
- Hon, T. et al. Highly accurate long-read HiFi sequencing data for five complex genomes. *Sci. Data* **7**, 399 (2020).
- Edger, P. P. et al. Origin and evolution of the octoploid strawberry genome. *Nat. Genet.* **51**, 541–547 (2019).
- Simão, F. A., Waterhouse, R. M., Ioannidis, P., Kriventseva, E. V. & Zdobnov, E. M. BUSCO: assessing genome assembly and annotation completeness with single-copy orthologs. *Bioinformatics* **31**, 3210–3212 (2015).
- Hizume, M., Kondo, T., Shibata, F. & Ishizuka, R. Flow cytometric determination of genome size in the Taxodiaceae, Cupressaceae *sensu stricto* and Sciadopityaceae. *Cytologia* **66**, 307–311 (2001).
- Gurevich, A., Saveliev, V., Vyahhi, N. & Tesler, G. QAST: quality assessment tool for genome assemblies. *Bioinformatics* **29**, 1072–1075 (2013).
- Chin, C.-S. et al. A diploid assembly-based benchmark for variants in the major histocompatibility complex. *Nat. Commun.* **11**, 4794 (2020).
- Li, H. Minimap2: pairwise alignment for nucleotide sequences. *Bioinformatics* **34**, 3094–3100 (2018).
- Li, H., Feng, X. & Chu, C. The design and construction of reference pangenome graphs with minigraph. *Genome Biol.* **21**, 265 (2020).
- Li, H. et al. A synthetic-diploid benchmark for accurate variant-calling evaluation. *Nat. Methods* **15**, 595–597 (2018).
- Zook, J. M. et al. An open resource for accurately benchmarking small variant and reference calls. *Nat. Biotechnol.* **37**, 561–566 (2019).
- Chaisson, M. J. P. et al. Multi-platform discovery of haplotype-resolved structural variation in human genomes. *Nat. Commun.* **10**, 1784 (2019).
- Cleary, J. G. et al. Comparing variant call files for performance benchmarking of next-generation sequencing variant calling pipelines. Preprint at *bioRxiv* <https://doi.org/10.1101/023754> (2015).

Publisher's note Springer Nature remains neutral with regard to jurisdictional claims in published maps and institutional affiliations.

© The Author(s), under exclusive licence to Springer Nature America, Inc. 2021

Methods

Haplotype-aware error correction. Hifiasm loads all reads into memory and performs all-versus-all pairwise alignment between them. For each read *R*, hifiasm effectively builds an approximate multisequence alignment from the pairwise alignment between *R* and each of its overlapping reads. Hifiasm then identifies positions on *R* at which there are two types of A/C/G/T bases in the alignment with each type supported by at least three overlapping reads. These positions inform base pair differences between haplotypes and are thus called informative positions. If *R* and its overlapping read *Q* are identical across all informative positions in the overlap, *Q* is regarded to come from the same haplotype as *R*. Hifiasm collects reads that are inferred to be on the same haplotype as *R* and use them to correct *R* with an algorithm similar to Falcon^{1,10}.

All-versus-all pairwise alignment is the major performance bottleneck in this step. Hifiasm uses a windowed version of the bit-vector algorithm by Myers et al.³³ to perform the base alignment. Instead of computing the alignment over the entire overlap, hifiasm splits read *R* into nonoverlapping windows and performs pairwise alignment in each window. This enables us to simultaneously align multiple windows using the SSE instructions³⁴. In practice, one potential issue with windowing is that the alignment around window boundaries may be unreliable. To alleviate this issue, hifiasm realigns the subregion around the window boundary if it sees mismatches or gaps within 20 bp around the boundary.

Constructing phased assembly graphs. After haplotype-aware error correction, most sequencing errors have been removed, while the marker positions are still kept. With nearly error-free reads, hifiasm can perform phasing accurately to determine if one overlap is among the reads coming from different haplotypes (that is, inconsistent overlap). The next step is to build the assembly string graph^{3,19}. In this graph, nodes represent oriented reads, and each edge between two nodes represents the overlap between the corresponding two reads. Note that only consistent overlaps are used to build the graph. Because hifiasm builds the graph on top of nearly error-free reads and highly accurate haplotype phasing, the produced assembly graph of hifiasm is simpler and cleaner than those of current assemblers for haploid genomes. However, for diploid genomes or polyploid genomes, its graph becomes more complicated as reads from different haplotypes are clearly separated out by phasing. Figure 1 shows an example. Since there is a heterozygous allele on reads in orange and blue, hifiasm separates them into two groups in which all reads in the same color belong to one group. Only the reads from same group are overlapped with each other. For reads in green, they are overlapped with the reads in both groups because the overlaps among them are not long enough to cover at least one heterozygous allele. As a result, hifiasm generates a bubble in the assembly graph. A bubble is a subgraph consisting of a single source node *v* and a single sink node *w* with more than one path between *v* and *w*, and all nodes in this bubble except *v* and *w* do not connect to the rest of the whole graph. Most existing assemblers aim to produce one contiguous contig from the graph (that is, single path in the graph) as much as possible. They tend to collapse bubbles when building the assembly graph. As a result, they will lose all but one allele in each bubble. In contrast, hifiasm is designed to retain all bubbles on the assembly graph. As there are still a few errors at the corrected reads, hifiasm adopts a topology-aware graph cleaning strategy. It first identifies substructures encoding local phasing information like bubbles, and then only cuts overlaps that are too short outside these substructures. Hifiasm additionally records the inconsistent overlaps, which are helpful in the following assembly construction steps.

Constructing a primary assembly. The construction of the primary assembly aims to produce contigs including one set of haplotypes but may switch subregions between haplotypes. In other words, each subregion in the primary assembly only comes from one haplotype, while the corresponding subregions of other haplotypes are removed as duplications. In this step, most existing assemblers follow the 'best overlap graph' strategy or its variants³⁵. Their key idea is to retain longer overlaps if there are multiple overlaps to a given read. In contrast, hifiasm produces a primary assembly mainly reliant on the graph topological structures and the phasing relationship among different haplotypes. Ideally, the phased assembly graph of hifiasm should be a chain of bubbles for diploid genomes (Fig. 2c). It is easy and reliable to extract a primary assembly from such a chain of bubbles by bubble popping³. However, there are still tips (that is, dead-end contigs broken in single end) on the assembly graph caused by broken bubbles due to lack of coverage, phasing errors or unresolvable repeats. To fix this problem, hifiasm proposes a three-stage procedure (Supplementary Fig. 1). First, each bubble in the graph is reduced into a single path using bubble popping. This step removes most duplicated subregions on different haplotypes without hampering the contiguity of primary assembly. Second, given a tip unitig *T* that is broken in one end but connected to a unitig *C* in another end, hifiasm checks if there are other unitigs, which are also connected to *C*, coming from the different haplotypes of *T*. If such unitigs are identified, hifiasm removes tip *T* so that unitig *C* will become longer. The reason is that for *T*, its corresponding region from different haplotypes has already been integrated into the new longer unitig *C*. Since hifiasm records inconsistent overlaps, it can check if two unitigs come from different haplotypes. Last, hifiasm uses the 'best overlap graph' strategy to deal with a few remaining unresolvable hard substructures on the assembly graph. In most cases, the graph

topological information and the phasing information is more reliable than only keeping the longer overlaps. As a result, hifiasm is able to generate a better primary assembly than current assemblers, which mainly rely on the 'best overlap graph' strategy.

Constructing a haplotype-resolved assembly. The phased assembly graph in hifiasm embeds the local phasing information that is resolvable with HiFi reads. In this graph, the corresponding node of a homozygous read is at a single path connecting two bubbles, while the corresponding node of a heterozygous read is at a bubble (Fig. 2). Given parental short reads, hifiasm labels child HiFi reads with the existing *k*-mer-based algorithm¹⁴. When generating a fully phased assembly for one haplotype, hifiasm drops reads of different haplotypes from the graph, while using the local phasing information in the graph to correct the mispartition of global phasing. Hifiasm does not drop reads at a single path connecting two bubbles, since these are homozygous reads that must be contained in both haplotypes. For a bubble in which all reads are heterozygous, hifiasm applies bubble popping to select a single best path consisting of the most reads with the expected haplotype label. If a few reads are assigned false labels by global phasing, they are likely to be corrected by the best path that traverses them. In addition, instead of dropping any read with a nonexpected haplotype label, hifiasm drops a contig if the haplotype labels of most reads in it are nonexpected.

Purging heterozygous duplications. In the primary assembly construction step, accurately keeping one set of haplotypes is more challenging for haplotype-resolved assemblers. Although the bubble-popping method and the tip-removing method of hifiasm already purge large numbers of duplications from multiple haplotypes, some duplications still remain on the primary assembly, especially for subregions with a high heterozygosity rate. Existing assemblers postprocess the primary assembly using downstream tools like purge_dups²⁰, which identify duplications by inexact all-versus-all contig alignment. If two contigs overlap with each other, the overlapped regions between them are duplications. However, inexact contig alignment might not be reliable on segmental duplications or repeats, leading to more duplications left or overpurged repetitive regions. To address this duplication challenge, hifiasm reassembles the contigs by building a string graph regarding contigs as nodes, called a purge graph. Given contig *A* and contig *B*, we define *A* as inconsistently overlapping *B* if there are enough reads of *A* that are inconsistently overlapped with the reads of *B*. Note that hifiasm records all inconsistent overlaps among reads in the initial phased assembly graph construction step by haplotype phasing. In the purge graph of hifiasm, each node is a contig, while an edge between two nodes is an inconsistent overlap between their corresponding contigs. Once the graph is built, hifiasm generates the nonredundant primary assembly by simple graph cleaning. As a result, the built-in purge duplication step of hifiasm is smoother and more reliable than existing downstream tools. This is because hifiasm identifies duplications from multiple haplotypes using accurate haplotype phasing of each read, while existing tools mainly rely on inexact contig alignment.

Evaluating collapsed misassemblies for inbred samples. We mapped HiFi reads with minimap2 (ref. 27) to each assembly and then called apparent heterozygous SNPs with htsbox, a fork of samtools. We selected biallelic SNPs such that each allele was supported by *d* reads, where *d* is set to 75% of the average coverage of the sample. We then hierarchically cluster these apparent SNPs²⁹ as follows: we merged two adjacent SNP clusters if (1) the minimum distance between them was within 10 kb, and (2) the density of SNPs in the merged cluster was at least 1 per 1 kb. A cluster longer than 5 kb and consisting of ≥10 SNPs was identified as a collapsed misassembly. Varying the thresholds changes the number of estimated misassemblies but does not alter the relative ranking between assemblers.

Evaluating gene completeness with asmgene. BUSCO³³ is a popular tool for evaluating gene completeness. It is very helpful for new species, but is underpowered for species with high-quality reference genomes. For example, BUSCO reports that the completeness of GRCh38 is only 94.8%, lower than the 95.2% completeness of the male HG002 hifiasm assembly (Supplementary Table 5).

To quantify gene completeness more accurately, we used the paf tools script from the minimap2 package²⁷ to calculate the asmgene scores. Unlike BUSCO, asmgene relies on a reference genome. It uses minimap2 to align Ensembl complementary DNAs (v99 for human and mouse and v47 for maize) to a reference genome or an assembly. For each transcript, asmgene records a hit if the transcript is mapped at ≥99% identity (≥97% for nonhuman species due to their higher diversity) over ≥99% of the transcript length. A transcript is considered a single-copy (SC) if it has only one hit; otherwise, it is considered to be multicopy (MC). The asmgene script chooses the longest transcript to represent a gene. In Tables 1 and 2, the percentage 'complete' equals $|\{ScorMCinASM\} \cap \{ScinREF\}| / |\{ScinREF\}|$, where $\{ScinREF\}$ denotes the set of single-copy genes in the reference genome and $\{ScorMCinASM\}$ denotes the union sets of single-copy and multicopy genes in the assembly. Similarly, the percentage 'duplicated' equals $|\{MCinASM\} \cap \{ScinREF\}| / |\{ScinREF\}|$. In Table 2, the percentage of 'multicopy gene retained' is calculated by $|\{MCinASM\} \cap \{MCinREF\}| / |\{MCinREF\}|$.

Reporting Summary. Further information on research design is available in the Nature Research Reporting Summary linked to this article.

Data availability

All HiFi data were obtained from the NCBI Sequence Read Archive: [SRR11606869](#) for *Z. mays*, [SRR11606870](#) for *M. musculus*, [SRR11606867](#) for *F. × ananassa*, [SRR11606868](#) and [SRR12048570](#) for *R. muscosa*, [SRP251156](#) for *S. semperivirens*, [SRR11292120–SRR11292123](#) for CHM13, [ERX3831682](#) for HG00733, and four runs ([SRR10382244](#), [SRR10382245](#), [SRR10382248](#) and [SRR10382249](#)) for HG002. For trio binning and computing QV, short reads were also downloaded: [SRR7782677](#) for HG00733, [ERR3241754](#) for HG00731 (father), [ERR3241755](#) for HG00732 (mother) and [SRX1082031](#) for CHM13. GIAB's 'homogeneity Run01' short-read runs were used for the HG002 trio. These HG002 reads were downsampled to 30-fold coverage. The BAC libraries of CHM13 and HG00733 can be found at <https://www.ncbi.nlm.nih.gov/nuccore/?term=VMRC59+and+complete/> and <https://www.ncbi.nlm.nih.gov/nuccore/?term=VMRC62+and+complete/>, respectively. The HG002 major histocompatibility complex reference sequences can be found at <https://github.com/NCBI-Hackathons/TheHumanPangenome/tree/master/MHC/assembly/MHCv1.1/> (ref. ²⁶). For BUSCO, the Embryophyta, Tetrapoda and Mammalia datasets are available at https://busco-data.ezlab.org/v4/data/lineages/embryophyta_odb10.2020-09-10.tar.gz, https://busco.ezlab.org/v2/datasets/tetrapoda_odb9.tar.gz and https://busco.ezlab.org/v2/datasets/mammalia_odb9.tar.gz, respectively. The CHM13 reference (v0.9) generated by the T2T consortium can be found at https://s3.amazonaws.com/nanopore-human-wgs/chm13/assemblies/chm13.draft_v0.9.fasta.gz. The hifiasm assemblies produced in this work are available at <https://zenodo.org/record/4393631> and <https://zenodo.org/record/4393750>.

Code availability

Hifiasm code is available at <https://github.com/chhyllp123/hifiasm/>.

References

33. Myers, G. A fast bit-vector algorithm for approximate string matching based on dynamic programming. *J. ACM* **46**, 395–415 (1999).

34. Cheng, H., Jiang, H., Yang, J., Xu, Y. & Shang, Y. BitMapper: an efficient all-mapper based on bit-vector computing. *BMC Bioinformatics* **16**, 192 (2015).
35. Miller, J. R. et al. Aggressive assembly of pyrosequencing reads with mates. *Bioinformatics* **24**, 2818–2824 (2008).

Acknowledgements

This study was supported by grants from the US National Institutes of Health (R01HG010040, U01HG010961 and U41HG010972 to H.L.).

Author contributions

H.C. and H.L. designed the algorithm, implemented hifiasm and drafted the manuscript. H.C. benchmarked hifiasm and other assemblers. G.T.C. ran hifiasm for *S. semperivirens*, HiCanu for *R. muscosa*, Peregrine for *S. semperivirens* and *R. muscosa*, and Falcon-Unzip for all datasets. X.F. helped with evaluation of the manuscript. H.Z. provided valuable suggestions for error correction and ran BUSCO.

Competing interests

G.T.C. is an employee of PacBio. H.L. is a consultant of Integrated DNA Technologies and on the Scientific Advisory Boards of Sentieon, BGI and OrigamiMed.

Additional information

Supplementary Information The online version contains supplementary material available at <https://doi.org/10.1038/s41592-020-01056-5>.

Correspondence and requests for materials should be addressed to H.L.

Peer review information *Nature Methods* thanks Benedict Paten and the other, anonymous, reviewer(s) for their contribution to the peer review of this work. Lin Tang was the primary editor on this article and managed its editorial process and peer review in collaboration with the rest of the editorial team.

Reprints and permissions information is available at www.nature.com/reprints.

Reporting Summary

Nature Research wishes to improve the reproducibility of the work that we publish. This form provides structure for consistency and transparency in reporting. For further information on Nature Research policies, see our [Editorial Policies](#) and the [Editorial Policy Checklist](#).

Statistics

For all statistical analyses, confirm that the following items are present in the figure legend, table legend, main text, or Methods section.

- | | |
|-------------------------------------|---|
| n/a | Confirmed |
| <input checked="" type="checkbox"/> | <input type="checkbox"/> The exact sample size (n) for each experimental group/condition, given as a discrete number and unit of measurement |
| <input checked="" type="checkbox"/> | <input type="checkbox"/> A statement on whether measurements were taken from distinct samples or whether the same sample was measured repeatedly |
| <input checked="" type="checkbox"/> | <input type="checkbox"/> The statistical test(s) used AND whether they are one- or two-sided
<i>Only common tests should be described solely by name; describe more complex techniques in the Methods section.</i> |
| <input checked="" type="checkbox"/> | <input type="checkbox"/> A description of all covariates tested |
| <input checked="" type="checkbox"/> | <input type="checkbox"/> A description of any assumptions or corrections, such as tests of normality and adjustment for multiple comparisons |
| <input checked="" type="checkbox"/> | <input type="checkbox"/> A full description of the statistical parameters including central tendency (e.g. means) or other basic estimates (e.g. regression coefficient) AND variation (e.g. standard deviation) or associated estimates of uncertainty (e.g. confidence intervals) |
| <input checked="" type="checkbox"/> | <input type="checkbox"/> For null hypothesis testing, the test statistic (e.g. F , t , r) with confidence intervals, effect sizes, degrees of freedom and P value noted
<i>Give P values as exact values whenever suitable.</i> |
| <input checked="" type="checkbox"/> | <input type="checkbox"/> For Bayesian analysis, information on the choice of priors and Markov chain Monte Carlo settings |
| <input checked="" type="checkbox"/> | <input type="checkbox"/> For hierarchical and complex designs, identification of the appropriate level for tests and full reporting of outcomes |
| <input checked="" type="checkbox"/> | <input type="checkbox"/> Estimates of effect sizes (e.g. Cohen's d , Pearson's r), indicating how they were calculated |

Our web collection on [statistics for biologists](#) contains articles on many of the points above.

Software and code

Policy information about [availability of computer code](#)

Data collection No software were used for data collection

Data analysis The manuscript describes the hifiasm assembly algorithm, which is free available at: <https://github.com/chhylp123/hifiasm>. We used hifiasm (v0.12), Falcon-Unzip (v1.8.1 for Falcon-kit & v1.3.7 for Falcon-unzip-kit), HiCanu (v2.1), Peregrine (v0.1.6.1) to generate different assemblies for comparison. Purge_dups (v1.2.3) was used to post-process assemblies of HiCanu. Mminimap2/paftools (r974), minigraph (r361), BUSCO (v3.0.2), dipcall (v0.1), QUAST (v5.0.2), dna-nn (r60), winnowmap (v1.11), Merqury (v1.1), htsbox (r345) and yak (r55) were used to evaluate all assemblies. BAC resolution of each assembly was measured by: <https://github.com/skoren/bacValidation>. The collapsed misassemblies for inbred samples were measured by the scripts at: <https://github.com/lh3/CHM-eval/blob/master/misc/clustreg.js>, and <https://github.com/lh3/CHM-eval/blob/master/misc/select-collapse-het.js>. All tools are open source and available at their corresponding repositories.

For manuscripts utilizing custom algorithms or software that are central to the research but not yet described in published literature, software must be made available to editors and reviewers. We strongly encourage code deposition in a community repository (e.g. GitHub). See the Nature Research [guidelines for submitting code & software](#) for further information.

Data

Policy information about [availability of data](#)

All manuscripts must include a [data availability statement](#). This statement should provide the following information, where applicable:

- Accession codes, unique identifiers, or web links for publicly available datasets
- A list of figures that have associated raw data
- A description of any restrictions on data availability

All HiFi data were obtained from NCBI Sequence Read Archive (SRA): SRR11606869 for Z. mays, SRR11606870 for M. musculus, SRR11606867 for F. x ananassa,

SRR11606868 and SRR12048570 for *R. muscosa*, SRP251156 for *S. sempervirens*, SRR11292120 through SRR11292123 for CHM13, ERX3831682 for HG00733, and four runs (SRR10382244, SRR10382245, SRR10382248 and SRR10382249) for HG002. For trio binning and computing QV, short reads were also downloaded: SRR7782677 for HG00733, ERR3241754 for HG00731 (father), ERR3241755 for HG00732 (mother) and SRX1082031 for CHM13. GIAB's "Homogeneity Run01" short-read runs were used for the HG002 trio. These HG002 reads were downsampled to 30-fold coverage. The BAC libraries of CHM13 and HG00733 can be found at <https://www.ncbi.nlm.nih.gov/nuccore/?term=VMRC59+and+complete> and <https://www.ncbi.nlm.nih.gov/nuccore/?term=VMRC62+and+complete>, respectively. The HG002 MHC reference sequences can be found at <https://github.com/NCBI-Hackathons/TheHumanPangenome/tree/master/MHC/assembly/MHCv1.1>. For BUSCO, the embryophyta dataset, the tetrapoda dataset and the mammalia dataset are available at https://busco-data.ezlab.org/v4/data/lineages/embryophyta_odb10.2020-09-10.tar.gz, http://busco.ezlab.org/v2/datasets/tetrapoda_odb9.tar.gz and http://busco.ezlab.org/v2/datasets/mammalia_odb9.tar.gz, respectively. The CHM13 reference (v0.9) generated by the T2T consortium can be found at https://s3.amazonaws.com/nanopore-human-wgs/chm13/assemblies/chm13.draft_v0.9.fasta.gz. The hifiasm assemblies produced in this work are available at <ftp://ftp.dfci.harvard.edu/pub/hli/hifiasm/submission/>.

Field-specific reporting

Please select the one below that is the best fit for your research. If you are not sure, read the appropriate sections before making your selection.

☒ Life sciences ☐ Behavioural & social sciences ☐ Ecological, evolutionary & environmental sciences

For a reference copy of the document with all sections, see [nature.com/documents/nr-reporting-summary-flat.pdf](https://www.nature.com/documents/nr-reporting-summary-flat.pdf)

Life sciences study design

All studies must disclose on these points even when the disclosure is negative.

Sample size	Not applicable since no statistical tests or power analyses were performed
Data exclusions	No data were excluded from analysis
Replication	Not applicable since this study only describes deterministic algorithms without statistic analysis
Randomization	Not applicable since this study introduces a method and does not include biological hypotheses analysis. All assembly algorithms are deterministic.
Blinding	Not applicable since this study does not involve statistic analysis and data acquisition

Reporting for specific materials, systems and methods

We require information from authors about some types of materials, experimental systems and methods used in many studies. Here, indicate whether each material, system or method listed is relevant to your study. If you are not sure if a list item applies to your research, read the appropriate section before selecting a response.

Materials & experimental systems

n/a	Involved in the study
<input checked="" type="checkbox"/>	<input type="checkbox"/> Antibodies
<input checked="" type="checkbox"/>	<input type="checkbox"/> Eukaryotic cell lines
<input checked="" type="checkbox"/>	<input type="checkbox"/> Palaeontology and archaeology
<input checked="" type="checkbox"/>	<input type="checkbox"/> Animals and other organisms
<input checked="" type="checkbox"/>	<input type="checkbox"/> Human research participants
<input checked="" type="checkbox"/>	<input type="checkbox"/> Clinical data
<input checked="" type="checkbox"/>	<input type="checkbox"/> Dual use research of concern

Methods

n/a	Involved in the study
<input checked="" type="checkbox"/>	<input type="checkbox"/> ChIP-seq
<input checked="" type="checkbox"/>	<input type="checkbox"/> Flow cytometry
<input checked="" type="checkbox"/>	<input type="checkbox"/> MRI-based neuroimaging